
Growing Q-Networks: Solving Continuous Control Tasks with Adaptive Control Resolution

Anonymous Author(s)

Affiliation

Address

email

Abstract

1 Recent reinforcement learning approaches have shown surprisingly strong capa-
2 bilities of bang-bang policies for solving continuous control benchmarks. The
3 underlying coarse action space discretizations often yield favorable exploration
4 characteristics, while final performance does not visibly suffer in the absence of
5 action penalization in line with optimal control theory. In robotics applications,
6 smooth control signals are commonly preferred to reduce system wear and im-
7 prove energy efficiency, while regularization via action costs can be detrimental to
8 exploration. Our work aims to bridge this performance gap by growing discrete
9 action spaces from coarse to fine control resolution. We take advantage of recent
10 results in decoupled Q-learning to scale our approach to high-dimensional action
11 spaces up to $\dim(\mathcal{A}) = 38$. Our work indicates that an adaptive control resolution
12 in combination with value decomposition yields simple critic-only algorithms that
13 enable surprisingly strong performance on continuous control tasks.

14 1 Introduction

15 Reinforcement learning for continuous control applications commonly leverages policies param-
16 eterized via continuous distributions. Recent works have shown surprisingly strong performance
17 of discrete policies in the actor-critic and critic-only setting [Tang and Agrawal, 2020, Tavakoli
18 et al., 2021, Seyde et al., 2021]. While discrete critic-only methods promise simpler controller
19 designs than their continuous actor-critic counterparts, applications such as robot control tend to
20 favor smooth control signals to maintain stability and prevent system wear [Hodel, 2018]. It has
21 previously been noted that coarse action discretization can provide exploration benefits early during
22 training [Czarnecki et al., 2018, Farquhar et al., 2020], while converged policies should increasingly
23 prioritize controller smoothness [Bohez et al., 2019].

24 Our work aims to bridge the gap between these two objectives while maintaining algorithm simplicity.
25 We introduce Growing Q-Networks (GQN), a simple discrete critic-only agent that combines the
26 scalability benefits of fully decoupled Q-learning [Seyde et al., 2022b] with the exploration benefits
27 of dynamic control resolution [Czarnecki et al., 2018, Farquhar et al., 2020]. Introducing an adaptive
28 action masking mechanism into a value-decomposed Q-Network, the agent can autonomously decide
29 when to increase control resolution. This approach enhances learning efficiency and balances
30 the exploration-exploitation trade-off more effectively, improving convergence speed and solution
31 smoothness. The primary contributions of this paper are threefold:

- 32 • **A framework for adaptive control resolution:** we grow control resolution from coarse to
33 fine within decoupled Q-learning. This reconciles coarse exploration during early training
34 with smooth control at convergence, retaining the scaling properties of decoupled control.

- 35 • **Insights into the scalability of discretized control:** our research provides valuable insights
36 into overcoming exploration challenges in soft-constrained continuous control settings via
37 simple discrete Q-learning methods, studying applicability in challenging control scenarios.
- 38 • **Comprehensive experimental validation:** we validate the effectiveness of our GQN
39 algorithm on a diverse set of continuous control tasks, highlighting the benefits of adaptive
40 control resolution over static DQN variations and recent continuous actor-critic methods.

41 The remainder of the paper is organized as follows: Section 2 reviews related work, Section 3
42 introduces preliminaries, Section 4 details the proposed GQN methodology, Section 5 presents
43 experimental results, and Section 6 concludes with a discussion on future research directions.

44 2 Related Works

45 In the following, we discuss several key related works grouped by their primary research thrust.

46 **Discretized Control** Learning continuous control tasks commonly relies on policies with continu-
47 ous support, primarily Gaussians with diagonal covariance matrices [Schulman et al., 2017, Haarnoja
48 et al., 2018, Abdolmaleki et al., 2018a, Hafner et al., 2020, Wulfmeier et al., 2020]. Recent works
49 have shown that competitive performance is often attainable via discrete policies [Tavakoli et al.,
50 2018, Neunert et al., 2020, Tang and Agrawal, 2020, Seyde et al., 2022a] with bang-bang control at
51 the extreme [Seyde et al., 2021]. Bang-bang controllers have been extensively investigated in optimal
52 control research [Sonneborn and Van Vleck, 1964, Bellman et al., 1956, LaSalle, 1959, Maurer
53 et al., 2005] as well as early works in reinforcement learning [Waltz and Fu, 1965, Lambert and
54 Levine, 1970, Anderson, 1988], while the extreme switching behavior was often observed to naturally
55 emerge even under continuous policy distributions [Huang et al., 2019, Novati and Koumoutsakos,
56 2019, Thuruthel et al., 2019]. The direct application of discrete action-space algorithms then harbors
57 potential benefits for reducing model complexity [Metz et al., 2017, Sharma et al., 2017, Tavakoli,
58 2021, Watkins and Dayan, 1992], although control resolution trade-offs and scalability may require
59 computational overhead [Van de Wiele et al., 2020].

60 **Scalability** The scalability of Q-learning approaches has been studied extensively in the context
61 of mitigating coordination challenges and system non-stationarity [Tan, 1993, Claus and Boutilier,
62 1998, Matignon et al., 2012, Lauer and Riedmiller, 2000, Matignon et al., 2007, Foerster et al., 2017,
63 Busoniu et al., 2006, Böhmer et al., 2019]. Exponential coupling can be avoided by information-
64 sharing [Schneider et al., 1999, Russell and Zimdars, 2003, Yang et al., 2018], composition of local
65 utility functions [Sunehag et al., 2017, Rashid et al., 2018, Son et al., 2019, Wang et al., 2020, Su et al.,
66 2021, Peng et al., 2021], and considering different levels of interaction [Guestrin et al., 2002, Kok and
67 Vlassis, 2006]. Centralization can further be facilitated via high degrees of parameter-sharing [Gupta
68 et al., 2017, Böhmer et al., 2020, Christianos et al., 2021, Van Seijen et al., 2017, Chu and Ye,
69 2017]). Decoupled control via Q-learning was proposed for Atari [Sharma et al., 2017] and extended
70 to mixing across higher-order action subspaces [Tavakoli et al., 2021], with decoupled bang-bang
71 control displaying strong performance on continuous control tasks [Seyde et al., 2022b]. While
72 coarse discretization can benefit exploration, particularly in the presence of action penalties, it may
73 also reduce steady-state performance. Conversely, fine discretization can exacerbate coordination
74 challenges [Seyde et al., 2022b, Ireland and Montana, 2024]. Here, we consider adapting the control
75 resolution over the course of training to achieve the best of both worlds.

76 **Expanding Action Spaces** Smith et al. [2023] present an adaptive policy regularization approach
77 that introduces soft constraints on feasible action regions, growing continuous regions linearly over
78 the course of training with adjustments based on dynamics uncertainty. They focus on learning
79 quadrupedal locomotion on hardware and expand locally around joint angles of a stable initial
80 pose. In discrete action spaces, one can instead leverage iterative resolution refinement. Czarnecki
81 et al. [2018] consider DeepMind Lab navigation tasks [Beattie et al., 2016] with a natively discrete
82 action space that avoids reasoning about system dynamics stability. Their policy-based method
83 formulates a mixture policy optimized under a distillation objective to facilitate knowledge transfer,
84 adjusting the mixing weights via Population Based Training (PBT) [Jaderberg et al., 2017]. Similarly,
85 Synnaeve et al. [2019] consider multi-agent coordination in StarCraft and adjust spatial command
86 resolution via PBT. Farquhar et al. [2020] grow action resolution under a linear growth schedule

87 while showing limited application to simple continuous control tasks, as they enumerate the action
 88 space and do not consider decoupled optimization. Beyond control applications, Yang et al. [2023]
 89 demonstrate adaptive mesh refinement strategies that reduce the errors in finite element simulations.
 90 Their refinement policy recursively adds finer elements, expanding the action space.

91 **Constrained Optimization** Reward-optimal bang-bang policies may not be desirable for real-world
 92 applications as they can be less energy efficient and increase wear and tear on physical systems,
 93 e.g., Hodel [2018]. In the past, this behavior was generally avoided by employing penalty functions
 94 as soft constraints at the cost of potentially hindering exploration or enabling reward hacking [Skalse
 95 et al., 2022]. The rewards and costs are automatically re-balanced to combat this issue in Bohez
 96 et al. [2019]. Similarly, undesirable behaviors are avoided by automatically balancing soft chance
 97 constraints with the primary rewards in Roy et al. [2021]. Here, we do not assume access to explicit
 98 penalty terms and efficiently learn controllers directly based on environment reward.

99 3 Preliminaries

100 We formulate the learning control problem as a Markov Decision Process (MDP) described by the
 101 tuple $\{\mathcal{S}, \mathcal{A}, \mathcal{T}, \mathcal{R}, \gamma\}$, where $\mathcal{S} \subset \mathbb{R}^N$ and $\mathcal{A} \subset \mathbb{R}^M$ denote the state and action space, respectively,
 102 $\mathcal{T} : \mathcal{S} \times \mathcal{A} \rightarrow \mathcal{S}$ the transition distribution, $\mathcal{R} : \mathcal{S} \times \mathcal{A} \rightarrow \mathbb{R}$ the reward function, and $\gamma \in [0, 1)$ the
 103 discount factor. Let s_t and a_t denote the state and action at time t , where actions are sampled from
 104 policy $\pi(a_t|s_t)$. We define the discounted infinite horizon return as $G_t = \sum_{\tau=t}^{\infty} \gamma^{\tau-t} R(s_\tau, a_\tau)$,
 105 where $s_{t+1} \sim \mathcal{T}(\cdot|s_t, a_t)$ and $a_t \sim \pi(\cdot|s_t)$. Our objective is to learn the optimal policy that
 106 maximizes the expected infinite horizon return $\mathbb{E}[G_t]$ under unknown dynamics and reward mappings.
 107 Conventional algorithms for continuous control settings leverage actor-critic designs with a continuous
 108 policy $\pi_\phi(a_t|s_t)$ maximizing expected returns from a value estimator $Q_\theta(s_t, a_t)$ or $V_\theta(s_t)$. Recent
 109 studies have shown strong results with simpler methods employing discretized actors [Tang and
 110 Agrawal, 2020, Seyde et al., 2021] or critic-only formulations [Tavakoli et al., 2018, 2021, Seyde
 111 et al., 2022b]. Here, we focus on the light-weight critic-only setting and increase control resolution
 112 over the course of training to bridge the gap between discrete and continuous control.

113 3.1 Deep Q-Networks

114 We consider the general framework of Deep Q-Networks (DQN) [Mnih et al., 2013], where the
 115 state-action value function $Q_\theta(s_t, a_t)$ is represented by a neural network with parameters θ . The
 116 parameters are updated to minimize the temporal-difference (TD) error, where we leverage several
 117 performance enhancements based on the Rainbow agent [Hessel et al., 2018]. These include target
 118 networks to improve stability in combination with double Q-learning to mitigate overestimation [Mnih
 119 et al., 2015, Van Hasselt et al., 2016], prioritized experience replay (PER) to focus sampling on more
 120 informative transitions [Schaul et al., 2015], and multi-step returns to improve stability of Bellman
 121 backups [Sutton and Barto, 2018]. The resulting objective function is given by

$$\mathcal{L}(\theta) = \sum_{b=1}^B L_\delta(y_t - Q_\theta(s_t, a_t)), \quad (1)$$

122 where action evaluation employs the target $y_t = \sum_{j=0}^{n-1} \gamma^j r(s_{t+j}, a_{t+j}) + \gamma^n Q_{\theta^-}(s_{t+n}, a_{t+n}^*)$,
 123 action selection uses $a_{t+1}^* = \arg \max_a Q_\theta(s_{t+1}, a)$, $L_\delta(\cdot)$ is the Huber loss and the batch size is B .
 124 Here, we leverage a target network with parameters Q_{θ^-} to further enhance learning stability.

125 3.2 Decoupled Q-Networks

126 Traditional DQN-based agents enumerate the entire action space and do not scale well to high
 127 dimensional control problems. Decoupled representations address scalability issues by treating
 128 subsets of action dimensions as separate agents and coordinating joint behavior in expectation [Sharma
 129 et al., 2017, Sunehag et al., 2017, Rashid et al., 2018, Tavakoli et al., 2021, Seyde et al., 2022b].
 130 The Decoupled Q-Networks (DecQN) agent introduced in Seyde et al. [2022b] employs a complete
 131 decomposition with the critic predicting univariate utilities for each action dimension a^j conditioned

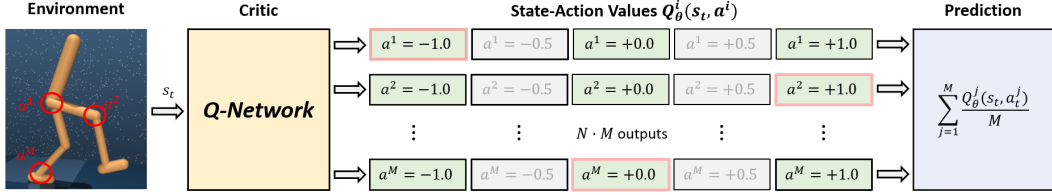


Figure 1: Schematic of a GQN agent with decoupled 5-bin discretization and 3-bin active subspace. The available actions are highlighted in green while the masked actions are depicted in gray. The predicted state-action values $Q(s, a^0, \dots, a^M)$ are computed via linear composition of the univariate utilities $Q(s, a^j)$ by selecting one action per dimension (red). We consider a homogeneous discretization across action dimensions for simplicity, heterogeneous discretization are also feasible.

132 on the global state s . The corresponding state-action value function is recovered as

$$Q_{\theta}(s_t, \mathbf{a}_t) = \sum_{j=1}^M \frac{Q_{\theta}^j(s_t, a_t^j)}{M}, \quad (2)$$

133 where the objective is analogous to Eq. 1, enabling centralized training with decentralized execution.

134 4 Growing Q-Networks

135 Discrete control algorithms have demonstrated competitive performance on continuous control
 136 benchmarks [Tang and Agrawal, 2020, Tavakoli et al., 2018, Seyde et al., 2021]. One potential benefit
 137 of these methods is the intrinsic coarse exploration that can accelerate the generation of informative
 138 environment feedback. Robot control applications favor smooth controllers at convergence to limit
 139 hardware stress. We aim to bridge the gap between coarse exploration capabilities and smooth control
 140 performance while retaining sample-efficient learning. We leverage insights from the growing action
 141 space literature [Czarnecki et al., 2018, Farquhar et al., 2020] and consider a decoupled critic that
 142 increases its control resolution over the course of training. To this end, we define the discrete action
 143 sub-space at iteration g as $\mathcal{A}^g \subset \mathcal{A}$ and modify the TD target to yield

$$y_t = \sum_{j=0}^{n-1} \gamma^j r(s_{t+j}, a_{t+j}) + \gamma^n \sum_{j=1}^M \max_{a_{t+n}^j \in \mathcal{A}^g} \frac{Q_{\theta}^j(s_{t+n}, a_{t+n}^j)}{M}, \quad (3)$$

144 where ϵ -greedy action sampling is constrained to \mathcal{A}^g . The network architecture accommodates the
 145 full discretized action space from the start and constrains the active set via action masking, enabling
 146 masked action combinations to profit from information propagation in the shared torso [Van Seijen
 147 et al., 2017]. A schematic of a decoupled agent with 5-bin discretization and active 3-bin subspace is
 148 provided in Figure 1. In order to deploy such an agent, we require a schedule for when to expand the
 149 active action space $\mathcal{A}^g \rightarrow \mathcal{A}^{g+1}$. Here, we consider two simple variations to limit engineering effort.
 150 First, we consider a linear schedule that doubles control resolution every $\frac{1}{N+1}$ of training episodes,
 151 where N indicates the number of subspaces \mathcal{A}^g . Second, we formulate an adaptive schedule based
 152 on an upper confidence bound inspired threshold over the moving average returns

$$G_{\text{threshold},t} = (1.00 - 0.05 \operatorname{sgn} \mu_{\text{MA},t-1}^G) \mu_{\text{MA},t-1}^G + 0.90 \sigma_{\text{MA},t-1}^G, \quad (4)$$

153 where μ_{MA} and σ_{MA} are the moving average mean and standard deviation of the evaluation returns,
 154 respectively. The objective underestimates the mean by 5% and expands the action space whenever
 155 the current mean return falls below the threshold $\mu_t^G < G_{\text{threshold},t}$, signifying performance stagnation.
 156 This parameterization can avoid pre-mature expansion when exploring under sparse rewards, but
 157 alternative formulations are also applicable. A qualitative example of our approach is provided in
 158 Figure 2, where we visualize the state-action value function over the course of training on a pendulum
 159 swing-up task. We consider a GQN agent with discretization $2 \rightarrow 9$ (meaning $\{2, 3, 5, 9\}$) and
 160 provide learned values for each action bin starting at initialization and adding a row every time the
 161 action space is grown (top to bottom). The active bins are framed in green, where we observe the
 162 accurate representation of the state-action value function for active bins, while the inactive bins still
 163 provide structured output due to the high degree of weight sharing provided by our architecture.

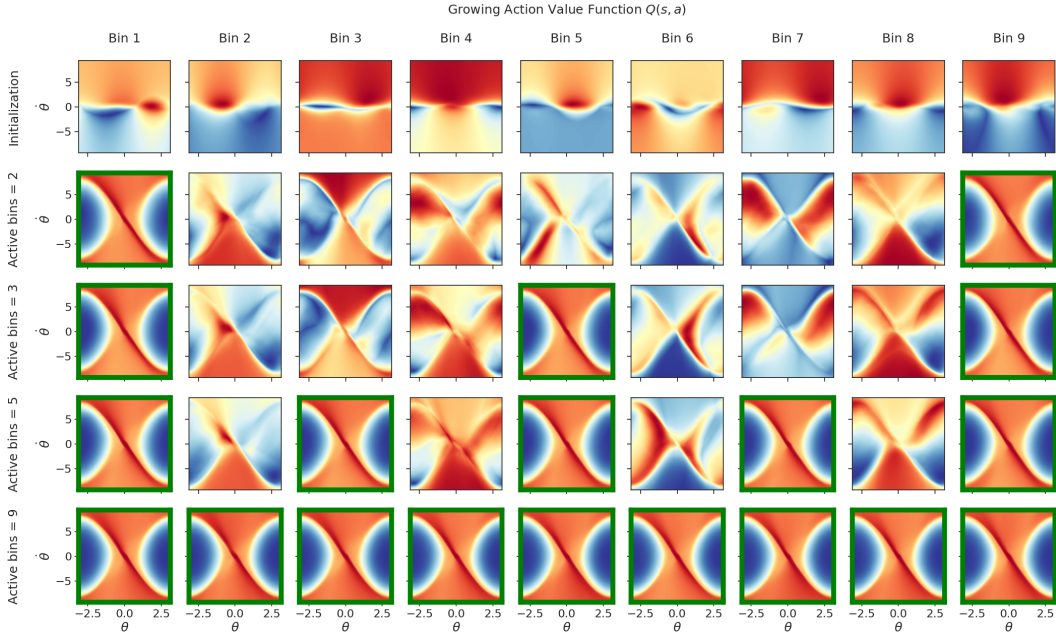


Figure 2: State-action values for a pendulum swing-up task over the course of training (top to bottom). The active bins are outlined in green. The value predictions transition from random at initialization to structured upon activation. Inactive bins profit from the emergent structure within the shared network torso to warm-start their optimization.

164 In the following section, we provide quantitative results on a range of challenging continuous control
 165 tasks. We use the same set of hyperparameters throughout all experiments, unless otherwise indicated,
 166 following the general parameterization of Seyde et al. [2022b] with a simple multi-layer perceptron
 167 architecture and dimensionality [512, 512]. We evaluate mean performance with standard deviation
 168 across 4 seeds and 10 evaluation episodes for each task. Our implementation builds on the codebase
 169 of Seyde et al. [2022b] and we provide hyperparameter values in Table 1 of the Appendix.

170 5 Experiments

171 We evaluate our approach on a selection of tasks from the DeepMind Control Suite [Tunyasuvunakool
 172 et al., 2020], MetaWorld [Yu et al., 2020], and MyoSuite [Vittorio et al., 2022]. The former two
 173 benchmarks generally do not consider action penalties and have previously been solved with bang-
 174 bang control [Seyde et al., 2022b]. Therefore, we focus on action-penalized task variations to
 175 encourage smooth control and highlight exploration challenges in the presence of penalty terms.

176 We first evaluate performance on tasks from the DeepMind Control Suite with action dimensionality
 177 up to $\dim(\mathcal{A}) = 38$. We consider 2 penalty weights $c_a \in \{0.1, 0.5\}$, such that rewards are computed
 178 as $r_t = r_t^o - c_a \sum_{j=1}^M a_t^{j2} / M$ from original reward r_t^o . We consider GQN agents that grow their
 179 action space discretization from 2 to 9 bins in each action dimension, where we evaluate both the
 180 linear and adaptive growing schedules discussed in Section 4. We compare performance against
 181 the state-of-the-art continuous control D4PG [Barth-Maroon et al., 2018] and DMPO [Abdolmaleki
 182 et al., 2018b] agents while providing two discrete control DecQN agents with stationary action space
 183 discretization of 2 or 9 for reference. The results in Figures 3 and 4 indicate the strong performance of
 184 GQN agents, with the adaptive schedule improving upon the linear schedule in terms of convergence
 185 rate and variance. Growing control resolution further provides a clear advantage over the stationary
 186 DecQN agents both in terms of final performance (vs. DecQN 2) and exploration abilities (vs. DecQN
 187 9). These observations mirror findings by Czarnecki et al. [2018], where coarse control resolution
 188 was beneficial for early exploration, a characteristic amplified by action penalties. We further observe
 189 strong performance of discrete GQN agents compared to the continuous D4PG and DMPO agents.

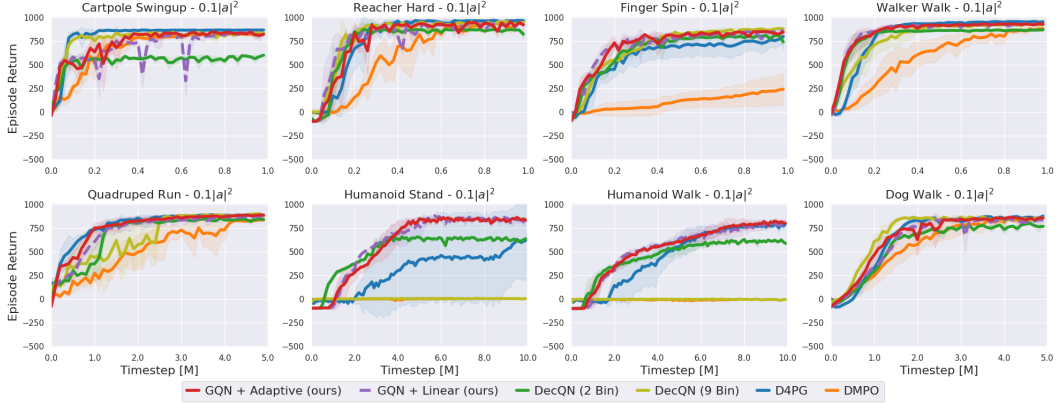


Figure 3: Performance on tasks from the DeepMind Control Suite with action penalty $-0.1|a|^2$. Our GQN agent grows its action space resolution via a $2 \rightarrow 3 \rightarrow 5 \rightarrow 9$ bin sequence, where the linear and adaptive expansion schedules yield similar results. The GQN agent performs competitive to the discrete DecQN as well as the continuous D4PG and DMPO baselines, achieving noticeable improvements on the Humanoid Stand and Walk tasks.

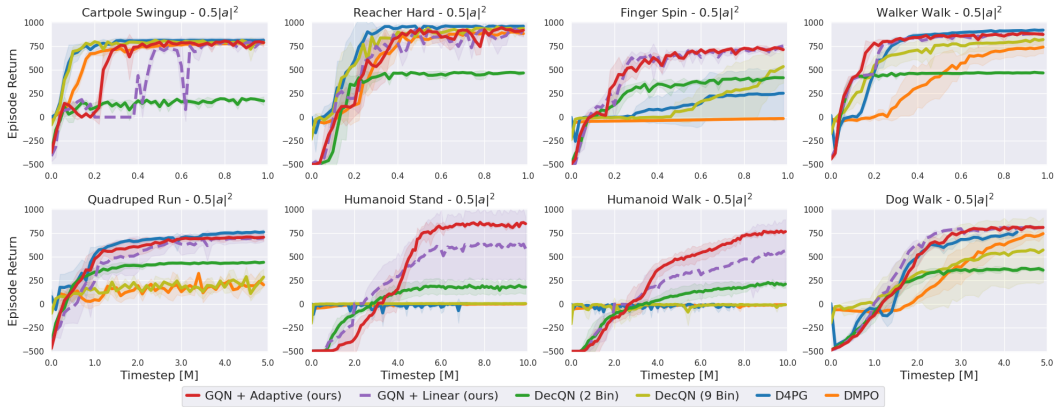


Figure 4: Performance on tasks from the DeepMind Control Suite with action penalty $-0.5|a|^2$. Our GQN agent grows its action space resolution via a $2 \rightarrow 3 \rightarrow 5 \rightarrow 9$ bin sequence, where we observe benefits of the adaptive variant over the linear schedule. GQN yields performance improvements over the discrete DecQN as well as the continuous D4PG and DMPO baselines, with particularly strong deltas on the Humanoid and Finger tasks.

190 The non-stationary optimization objective inherent to GQN may not be necessary on simpler tasks
 191 with limited exploration requirements such as Cartpole Swinup or Reacher Hard, while it significantly
 192 improves performance on complex domains such as Humanoid or Dog.

193 In order to provide additional quantitative motivation for the presence of action penalties, we compare
 194 the smoothness of the converged policies in Figure 5. We consider the adaptive GQN agent with
 195 action penalties $c_a \in \{0.1, 0.5\}$ and the continuous D4PG agent with action penalty $c_a = 0.5$. The
 196 metrics we consider are original non-penalized task performance, R , incurred action penalty, P ,
 197 action magnitude, $|a|$, instantaneous action change, $|\Delta a|$, and the Fast Fourier Transform (FFT) based
 198 smoothness metric from Mysore et al. [2021], SM . All metrics are normalized by the corresponding
 199 value achieved by the unconstrained GQN agent with $c_a = 0.0$. The results indicate that increasing
 200 the action penalty yields noticeably smoother control signals while only having a minor impact on
 201 the original task performance as measured by the unconstrained reward, R . We further find that
 202 the smoothness of the discrete GQN agent is at least as good as for the continuous D4PG agent on the
 203 tasks considered (note that D4PG is unable to solve the Humanoid tasks, $R \approx 0$).

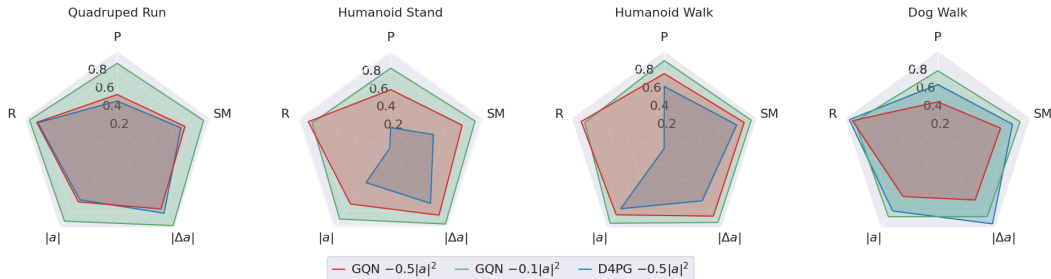


Figure 5: Comparison of control smoothness and reward performance, relative to GQN without action penalties. Increasing the action penalty coefficient yields smoother control while only having a minor impact on the original task performance as measured by unconstrained reward R . The discrete GQN further improves upon the continuous D4PG agent.

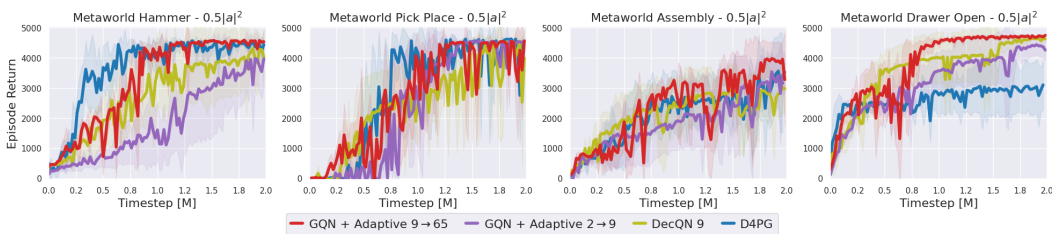


Figure 6: Performance on manipulation tasks from MetaWorld with action penalty $-0.5|a|^2$. These tasks require control at the velocity level and are therefore more challenging to solve with extremely coarse discretization. We therefore investigate the scalability of our GQN agent and consider growing discretizations via a $9 \rightarrow 17 \rightarrow 33 \rightarrow 65$ bin sequence. The resulting policy achieves stable learning and performs competitively with the continuous D4PG baseline while improving on the stationary 9 bins DecQN agent.

204 Next, we extend our study to velocity-level control tasks for the Sawyer robot in MetaWorld. While
 205 acceleration-level control often provides sufficient filtering to interact favorably with highly dis-
 206 cretized bang-bang exploration, velocity-level control tends to require more fine-grained inputs. We
 207 investigate the scalability of growing action spaces within decoupled Q-learning representations. To
 208 this end, we consider GQN agents with $2 \rightarrow 9$ and $9 \rightarrow 65$ (meaning $\{9, 17, 33, 65\}$) discretization as
 209 well as a stationary DecQN agent with 9 bins. The results in Figure 6 indicate that initial bang-bang
 210 action selection is not well-suited for generating velocity-level actions, with the agent achieving
 211 good performance once transitioning to more fine-grained discretization (GQN $2 \rightarrow 9$). Interestingly,
 212 considering a larger growing action space with GQN $9 \rightarrow 65$ can surpass the performance of a
 213 stationary DecQN 9 agent, despite the non-stationary optimization objective induced by the addition
 214 of finer action discretizations over the course of training. The performance of GQN $9 \rightarrow 65$ is
 215 furthermore competitive with the continuous D4PG agent on average.

216 Lastly, we stress-test our approach by considering a selection of tasks from the MyoSuite benchmark.
 217 The tasks require control of biomechanical models that aim to be physiologically accurate with
 218 $\dim(\mathcal{A}) = 39$ and up to $\dim(\mathcal{O}) = 115$ and should constrain the applicability of simple decoupled
 219 Q-learning approaches such as GQN. Indeed, we find that the agent capacity becomes a limiting
 220 factor yielding overestimation errors further exacerbated by the large magnitude reward signals. We
 221 therefore extend the network capacity to $[512, 512] \rightarrow [2048, 2048]$ and lower the discount factor
 222 $\gamma = 0.99 \rightarrow 0.95$ (alternatively, increasing multi-step returns $3 \rightarrow 5$ worked similarly well). With
 223 these parameter adjustments, we observe good performance as measured by task success at the final
 224 step of an episode, comparing favorably to the continuous D4PG agent in Figure 7. This further
 225 underlines the surprising effectiveness that decoupled discrete control can yield in continuous control
 226 settings and the benefit of adaptive control resolution change over the course of training.

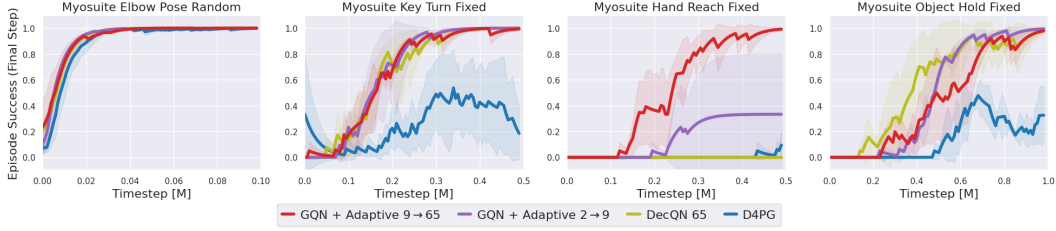


Figure 7: Performance for controlling biomechanical models from the MyoSuite as measured by task success at termination. These continuous control tasks stress test growing decoupled discrete action spaces, due to their dimensionality and inherent complexity. Increasing the network capacity and adjusting the discount factor to mitigate overestimation, we observe strong performance for growing action spaces up to a discretization of 65 bins.

227 6 Conclusion

228 This work investigates the application of growing action spaces within decoupled Q-learning to
 229 efficiently solve continuous control tasks. Our Growing Q-Networks (GQN) agent leverages a linear
 230 value decomposition along actuators to retain scalability in high-dimensional action spaces and adap-
 231 tively increases control resolution over the course of training. This enables coarse exploration early
 232 during training without reduced control smoothness and accuracy at convergence. The resulting agent
 233 is robust and performs well even for very fine control resolutions despite inherent non-smoothness
 234 in the optimization objective arising at the transition between resolution levels. While GQN as a
 235 critic-only method displays very strong performance compared to recent continuous actor-critic
 236 methods on the tasks considered, we also investigate scenarios that prove challenging for decoupled
 237 discrete controllers as exemplified by velocity-level control of simulated manipulators or applications
 238 to control of biomechanical models. Interesting avenues for future work include addressing coordina-
 239 tion challenges in increasingly high-dimensional action spaces and mitigating overestimation bias.
 240 Generally, GQN provides a simple yet capable agent that efficiently bridges the gap between coarse
 241 exploration and solution smoothness through adaptive control resolution refinement.

242 References

- 243 A. Abdolmaleki, J. T. Springenberg, J. Degraeve, S. Bohez, Y. Tassa, D. Belov, N. Heess, and
 244 M. Riedmiller. Relative entropy regularized policy iteration. *arXiv preprint arXiv:1812.02256*,
 245 2018a.
- 246 A. Abdolmaleki, J. T. Springenberg, Y. Tassa, R. Munos, N. Heess, and M. Riedmiller. Maximum a
 247 posteriori policy optimisation. *arXiv preprint arXiv:1806.06920*, 2018b.
- 248 C. W. Anderson. Learning to Control an Inverted Pendulum with Connectionist Networks. In
 249 *Proceedings of the American Control Conference (ACC)*, 1988.
- 250 G. Barth-Maroon, M. W. Hoffman, D. Budden, W. Dabney, D. Horgan, D. Tb, A. Muldal, N. Heess,
 251 and T. Lillicrap. Distributed distributional deterministic policy gradients. *arXiv preprint*
 252 *arXiv:1804.08617*, 2018.
- 253 C. Beattie, J. Z. Leibo, D. Teplyashin, T. Ward, M. Wainwright, H. Küttler, A. Lefrancq, S. Green,
 254 V. Valdés, A. Sadik, et al. Deepmind lab. *arXiv preprint arXiv:1612.03801*, 2016.
- 255 R. Bellman, I. Glicksberg, and O. Gross. On the “bang-bang” control problem. *Quarterly of Applied*
 256 *Mathematics*, 14(1), 1956.
- 257 S. Bohez, A. Abdolmaleki, M. Neunert, J. Buchli, N. Heess, and R. Hadsell. Value constrained
 258 model-free continuous control. *arXiv preprint arXiv:1902.04623*, 2019.
- 259 W. Böhmer, T. Rashid, and S. Whiteson. Exploration with unreliable intrinsic reward in multi-agent
 260 reinforcement learning. *arXiv preprint arXiv:1906.02138*, 2019.

- 261 W. Böhmer, V. Kurin, and S. Whiteson. Deep coordination graphs. In *International Conference on*
262 *Machine Learning*, pages 980–991. PMLR, 2020.
- 263 L. Busoniu, B. De Schutter, and R. Babuska. Decentralized reinforcement learning control of a
264 robotic manipulator. In *2006 9th International Conference on Control, Automation, Robotics and*
265 *Vision*, pages 1–6. IEEE, 2006.
- 266 F. Christianos, G. Papoudakis, M. A. Rahman, and S. V. Albrecht. Scaling multi-agent reinforcement
267 learning with selective parameter sharing. In *International Conference on Machine Learning*,
268 pages 1989–1998. PMLR, 2021.
- 269 X. Chu and H. Ye. Parameter sharing deep deterministic policy gradient for cooperative multi-agent
270 reinforcement learning. *arXiv preprint arXiv:1710.00336*, 2017.
- 271 C. Claus and C. Boutilier. The dynamics of reinforcement learning in cooperative multiagent systems.
272 *AAAI/IAAI*, 1998:2, 1998.
- 273 W. Czarnecki, S. Jayakumar, M. Jaderberg, L. Hasenclever, Y. W. Teh, N. Heess, S. Osindero, and
274 R. Pascanu. Mix & match agent curricula for reinforcement learning. In *International Conference*
275 *on Machine Learning*, pages 1087–1095. PMLR, 2018.
- 276 G. Farquhar, L. Gustafson, Z. Lin, S. Whiteson, N. Usunier, and G. Synnaeve. Growing action spaces.
277 In *International Conference on Machine Learning*, pages 3040–3051. PMLR, 2020.
- 278 J. Foerster, N. Nardelli, G. Farquhar, T. Afouras, P. H. Torr, P. Kohli, and S. Whiteson. Stabilising
279 experience replay for deep multi-agent reinforcement learning. In *International conference on*
280 *machine learning*, pages 1146–1155. PMLR, 2017.
- 281 C. Guestrin, M. Lagoudakis, and R. Parr. Coordinated reinforcement learning. In *ICML*, volume 2,
282 pages 227–234. Citeseer, 2002.
- 283 J. K. Gupta, M. Egorov, and M. Kochenderfer. Cooperative multi-agent control using deep reinforce-
284 ment learning. In *International conference on autonomous agents and multiagent systems*, pages
285 66–83. Springer, 2017.
- 286 T. Haarnoja, A. Zhou, K. Hartikainen, G. Tucker, S. Ha, J. Tan, V. Kumar, H. Zhu, A. Gupta,
287 P. Abbeel, et al. Soft actor-critic algorithms and applications. *arXiv preprint arXiv:1812.05905*,
288 2018.
- 289 D. Hafner, T. Lillicrap, M. Norouzi, and J. Ba. Mastering atari with discrete world models. *arXiv*
290 *preprint arXiv:2010.02193*, 2020.
- 291 M. Hessel, J. Modayil, H. Van Hasselt, T. Schaul, G. Ostrovski, W. Dabney, D. Horgan, B. Piot,
292 M. Azar, and D. Silver. Rainbow: Combining improvements in deep reinforcement learning. In
293 *Thirty-second AAAI conference on artificial intelligence*, 2018.
- 294 B. J. Hodel. Learning to Operate an Excavator via Policy Optimization. *Procedia Computer Science*,
295 140, 2018.
- 296 S. H. Huang, M. Zambelli, J. Kay, M. F. Martins, Y. Tassa, P. M. Pilarski, and R. Hadsell.
297 Learning Gentle Object Manipulation with Curiosity-Driven Deep Reinforcement Learning.
298 *arXiv:1903.08542*, 2019.
- 299 D. Ireland and G. Montana. Revalued: Regularised ensemble value-decomposition for factorisable
300 markov decision processes. *arXiv preprint arXiv:2401.08850*, 2024.
- 301 M. Jaderberg, V. Dalibard, S. Osindero, W. M. Czarnecki, J. Donahue, A. Razavi, O. Vinyals,
302 T. Green, I. Dunning, K. Simonyan, et al. Population based training of neural networks. *arXiv*
303 *preprint arXiv:1711.09846*, 2017.
- 304 J. R. Kok and N. Vlassis. Collaborative multiagent reinforcement learning by payoff propagation.
305 *Journal of Machine Learning Research*, 7:1789–1828, 2006.
- 306 J. Lambert and M. Levine. A two-stage learning control system. *Trans. on Automatic Control*, 15(3),
307 1970.

- 308 J. P. LaSalle. Time Optimal Control Systems. *Proceedings of the National Academy of Sciences*, 45
309 (4), 1959.
- 310 M. Lauer and M. Riedmiller. An algorithm for distributed reinforcement learning in cooperative
311 multi-agent systems. In *In Proceedings of the Seventeenth International Conference on Machine*
312 *Learning*. Citeseer, 2000.
- 313 L. Matignon, G. J. Laurent, and N. Le Fort-Piat. Hysteretic q-learning: an algorithm for decentral-
314 ized reinforcement learning in cooperative multi-agent teams. In *2007 IEEE/RSJ International*
315 *Conference on Intelligent Robots and Systems*, pages 64–69. IEEE, 2007.
- 316 L. Matignon, G. J. Laurent, and N. Le Fort-Piat. Independent reinforcement learners in cooperative
317 markov games: a survey regarding coordination problems. *The Knowledge Engineering Review*,
318 27:1–31, 2012.
- 319 H. Maurer, C. Büskens, J.-H. R. Kim, and C. Y. Kaya. Optimization methods for the verification
320 of second order sufficient conditions for bang–bang controls. *Optimal Control Applications and*
321 *Methods*, 26(3), 2005.
- 322 L. Metz, J. Ibarz, N. Jaitly, and J. Davidson. Discrete sequential prediction of continuous actions for
323 deep rl. *arXiv preprint arXiv:1705.05035*, 2017.
- 324 V. Mnih, K. Kavukcuoglu, D. Silver, A. Graves, I. Antonoglou, D. Wierstra, and M. Riedmiller.
325 Playing atari with deep reinforcement learning. *arXiv preprint arXiv:1312.5602*, 2013.
- 326 V. Mnih, K. Kavukcuoglu, D. Silver, A. A. Rusu, J. Veness, M. G. Bellemare, A. Graves, M. Ried-
327 miller, A. K. Fidjeland, G. Ostrovski, et al. Human-level control through deep reinforcement
328 learning. *nature*, 518:529–533, 2015.
- 329 S. Mysore, B. Mabsout, R. Mancuso, and K. Saenko. Regularizing action policies for smooth control
330 with reinforcement learning. In *2021 IEEE International Conference on Robotics and Automation*
331 *(ICRA)*, pages 1810–1816. IEEE, 2021.
- 332 M. Neunert, A. Abdolmaleki, M. Wulfmeier, T. Lampe, T. Springenberg, R. Hafner, F. Romano,
333 J. Buchli, N. Heess, and M. Riedmiller. Continuous-discrete reinforcement learning for hybrid
334 control in robotics. In *Conference on Robot Learning*, pages 735–751. PMLR, 2020.
- 335 G. Novati and P. Koumoutsakos. Remember and Forget for Experience Replay. In *International*
336 *Conference on Machine Learning (ICML)*, 2019.
- 337 B. Peng, T. Rashid, C. Schroeder de Witt, P.-A. Kamienny, P. Torr, W. Böhmer, and S. Whiteson.
338 Facmac: Factored multi-agent centralised policy gradients. *Advances in Neural Information*
339 *Processing Systems*, 34, 2021.
- 340 T. Rashid, M. Samvelyan, C. Schroeder, G. Farquhar, J. Foerster, and S. Whiteson. Qmix: Mono-
341 tonic value function factorisation for deep multi-agent reinforcement learning. In *International*
342 *Conference on Machine Learning*, pages 4295–4304. PMLR, 2018.
- 343 J. Roy, R. Girgis, J. Romoff, P.-L. Bacon, and C. Pal. Direct behavior specification via constrained
344 reinforcement learning. *arXiv preprint arXiv:2112.12228*, 2021.
- 345 S. J. Russell and A. Zimdars. Q-decomposition for reinforcement learning agents. In *Proceedings of*
346 *the 20th International Conference on Machine Learning (ICML-03)*, pages 656–663, 2003.
- 347 T. Schaul, J. Quan, I. Antonoglou, and D. Silver. Prioritized experience replay. *arXiv preprint*
348 *arXiv:1511.05952*, 2015.
- 349 J. G. Schneider, W.-K. Wong, A. W. Moore, and M. A. Riedmiller. Distributed value functions. In
350 *ICML*, 1999.
- 351 J. Schulman, F. Wolski, P. Dhariwal, A. Radford, and O. Klimov. Proximal policy optimization
352 algorithms. *arXiv preprint arXiv:1707.06347*, 2017.

- 353 T. Seyde, I. Gilitschenski, W. Schwarting, B. Stellato, M. Riedmiller, M. Wulfmeier, and D. Rus. Is
354 bang-bang control all you need? solving continuous control with bernoulli policies. *Advances in*
355 *Neural Information Processing Systems*, 34, 2021.
- 356 T. Seyde, W. Schwarting, I. Gilitschenski, M. Wulfmeier, and D. Rus. Strength through diversity:
357 Robust behavior learning via mixture policies. In *Conference on Robot Learning*, pages 1144–1155.
358 PMLR, 2022a.
- 359 T. Seyde, P. Werner, W. Schwarting, I. Gilitschenski, M. Riedmiller, D. Rus, and M. Wulfmeier.
360 Solving continuous control via q-learning. In *The Eleventh International Conference on Learning*
361 *Representations*, 2022b.
- 362 S. Sharma, A. Suresh, R. Ramesh, and B. Ravindran. Learning to factor policies and action-value
363 functions: Factored action space representations for deep reinforcement learning. *arXiv preprint*
364 *arXiv:1705.07269*, 2017.
- 365 J. Skalse, N. Howe, D. Krasheninnikov, and D. Krueger. Defining and characterizing reward gaming.
366 *Advances in Neural Information Processing Systems*, 35:9460–9471, 2022.
- 367 L. Smith, Y. Cao, and S. Levine. Grow your limits: Continuous improvement with real-world rl for
368 robotic locomotion. *arXiv preprint arXiv:2310.17634*, 2023.
- 369 K. Son, D. Kim, W. J. Kang, D. E. Hostallero, and Y. Yi. Qtran: Learning to factorize with
370 transformation for cooperative multi-agent reinforcement learning. In *International Conference on*
371 *Machine Learning*, pages 5887–5896. PMLR, 2019.
- 372 L. M. Sonneborn and F. S. Van Vleck. The Bang-Bang Principle for Linear Control Systems. *Journal*
373 *of the Society for Industrial and Applied Mathematics Series A Control*, 2(2), 1964.
- 374 J. Su, S. Adams, and P. A. Beling. Value-decomposition multi-agent actor-critics. In *Proceedings of*
375 *the AAAI Conference on Artificial Intelligence*, volume 35, pages 11352–11360, 2021.
- 376 P. Sunehag, G. Lever, A. Gruslys, W. M. Czarnecki, V. Zambaldi, M. Jaderberg, M. Lanctot, N. Son-
377 nerat, J. Z. Leibo, K. Tuyls, et al. Value-decomposition networks for cooperative multi-agent
378 learning. *arXiv preprint arXiv:1706.05296*, 2017.
- 379 R. S. Sutton and A. G. Barto. *Reinforcement learning: An introduction*. 2018.
- 380 G. Synnaeve, J. Gehring, Z. Lin, D. Haziza, N. Usunier, D. Rothmel, V. Mella, D. Ju, N. Carion,
381 L. Gustafson, et al. Growing up together: Structured exploration for large action spaces. 2019.
- 382 M. Tan. Multi-agent reinforcement learning: Independent vs. cooperative agents. In *Proceedings of*
383 *the tenth international conference on machine learning*, pages 330–337, 1993.
- 384 Y. Tang and S. Agrawal. Discretizing continuous action space for on-policy optimization. In
385 *Proceedings of the AAAI Conference on Artificial Intelligence*, volume 34, pages 5981–5988, 2020.
- 386 A. Tavakoli. *On structural and temporal credit assignment in reinforcement learning*. PhD thesis,
387 Imperial College London, 2021.
- 388 A. Tavakoli, F. Pardo, and P. Kormushev. Action branching architectures for deep reinforcement
389 learning. In *Proceedings of the AAAI Conference on Artificial Intelligence*, volume 32, 2018.
- 390 A. Tavakoli, M. Fatemi, and P. Kormushev. Learning to represent action values as a hypergraph on
391 the action vertices. In *International Conference on Learning Representations*, 2021.
- 392 T. G. Thuruthel, E. Falotico, F. Renda, and C. Laschi. Model-Based Reinforcement Learning for
393 Closed-Loop Dynamic Control of Soft Robotic Manipulators. *IEEE T-RO*, 35(1), 2019.
- 394 S. Tunyasuvunakool, A. Muldal, Y. Doron, S. Liu, S. Bohez, J. Merel, T. Erez, T. Lillicrap, N. Heess,
395 and Y. Tassa. dm_control: Software and tasks for continuous control. *Software Impacts*, 6:100022,
396 2020.
- 397 T. Van de Wiele, D. Warde-Farley, A. Mnih, and V. Mnih. Q-learning in enormous action spaces via
398 amortized approximate maximization. *arXiv preprint arXiv:2001.08116*, 2020.

- 399 H. Van Hasselt, A. Guez, and D. Silver. Deep reinforcement learning with double q-learning. In
400 *Proceedings of the AAAI conference on artificial intelligence*, volume 30, 2016.
- 401 H. Van Seijen, M. Fatemi, J. Romoff, R. Laroche, T. Barnes, and J. Tsang. Hybrid reward architecture
402 for reinforcement learning. *Advances in Neural Information Processing Systems*, 30, 2017.
- 403 C. Vittorio, W. Huawei, D. Guillaume, S. Massimo, and K. Vikash. Myosuite – a contact-rich simula-
404 tion suite for musculoskeletal motor control. <https://github.com/myohub/myosuite>,
405 2022. URL <https://arxiv.org/abs/2205.13600>.
- 406 M. Waltz and K. Fu. A heuristic approach to reinforcement learning control systems. *IEEE TACON*,
407 10(4), 1965.
- 408 Y. Wang, B. Han, T. Wang, H. Dong, and C. Zhang. Dop: Off-policy multi-agent decomposed policy
409 gradients. In *International Conference on Learning Representations*, 2020.
- 410 C. J. Watkins and P. Dayan. Q-learning. *Machine learning*, 8:279–292, 1992.
- 411 M. Wulfmeier, A. Abdolmaleki, R. Hafner, J. T. Springenberg, M. Neunert, N. Siegel, T. Hertweck,
412 T. Lampe, N. Heess, and M. Riedmiller. Compositional Transfer in Hierarchical Reinforcement
413 Learning. In *Robotics: Science and Systems (RSS)*, 2020.
- 414 J. Yang, T. Dzanic, B. Petersen, J. Kudo, K. Mittal, V. Tomov, J.-S. Camier, T. Zhao, H. Zha, T. Kolev,
415 et al. Reinforcement learning for adaptive mesh refinement. In *International Conference on*
416 *Artificial Intelligence and Statistics*, pages 5997–6014. PMLR, 2023.
- 417 Y. Yang, R. Luo, M. Li, M. Zhou, W. Zhang, and J. Wang. Mean field multi-agent reinforcement
418 learning. In *International Conference on Machine Learning*, pages 5571–5580. PMLR, 2018.
- 419 T. Yu, D. Quillen, Z. He, R. Julian, K. Hausman, C. Finn, and S. Levine. Meta-world: A benchmark
420 and evaluation for multi-task and meta reinforcement learning. In *Conference on Robot Learning*,
421 pages 1094–1100. PMLR, 2020.

422 A Hyperparameters

423 Throughout our experiments, we use the hyperparameter values in Table 1 unless otherwise indicated.

Table 1: GQN hyperparameters.

Parameter	Value
Optimizer	Adam
Learning rate	1×10^{-4}
n -step returns	3
Action repeat	1
Discount γ	0.99
Batch size	256
Gradient clipping	40
Target update period	100
Imp. sampling exponent	0.2
Priority exponent	0.6
Exploration ϵ	0.1

424